PLOS ONE

Changes in the gut microbiota of NOD mice in response to an oral *Salmonella*-based vaccine against type 1 diabetes

Jacob Cobb[1], Sameh S. M. Soliman[2,3], Mauricio Retuerto[4], Janine C. Quijano[1], Chris Orr[1], Mahmoud Ghannoum[4], Fouad Kandeel[1], Mohamed I. Husseiny[1,5]*

1 Department of Translational Research & Cellular Therapeutics, Arthur Riggs Diabetes & Metabolism Research Institute, Beckman Research Institute, City of Hope National Medical Center, Duarte, California, United States of America, 2 Research Institute for Medical and Health Sciences, University of Sharjah, Sharjah, United Arab Emirates, 3 Department of Medicinal Chemistry, College of Pharmacy, University of Sharjah, Sharjah, United Arab Emirates, 4 Center for Medical Mycology, Department of Dermatology, University Hospitals Cleveland Medical Center, Case Western Reserve University, Cleveland, Ohio, United States of America, 5 Faculty of Pharmacy, Zagazig University, Zagazig, Egypt

* melsayed@coh.org

Abstract

We developed an oral *Salmonella*-based vaccine that prevents and reverses diabetes in non-obese diabetic (NOD) mice. Related to this, the gastrointestinal tract harbors a complex dynamic population of microorganisms, the gut microbiome, that influences host homeostasis and metabolism. Changes in the gut microbiome are associated with insulin dysfunction and type 1 diabetes (T1D). Oral administration of diabetic autoantigens as a vaccine can restore immune balance. However, it was not known if a *Salmonella*-based vaccine would impact the gut microbiome. We administered a *Salmonella*-based vaccine to prediabetic NOD mice. Changes in the gut microbiota and associated metabolome were assessed using next-generation sequencing and gas chromatography-mass spectrometry (GC-MS). The *Salmonella*-based vaccine did not cause significant changes in the gut microbiota composition immediately after vaccination although at 30 days post-vaccination changes were seen. Additionally, no changes were noted in the fecal mycobiome between vaccine- and control/vehicle-treated mice. Significant changes in metabolic pathways related to inflammation and proliferation were found after vaccine administration. The results from this study suggest that an oral *Salmonella*-based vaccine alters the gut microbiome and metabolome towards a more tolerant composition. These results support the use of orally administered *Salmonella*-based vaccines that induced tolerance after administration.

Introduction

Type 1 diabetes (T1D) is characterized by autoimmune-mediated destruction of insulin-secreting pancreatic β-cells. Preproinsulin (PPI) is likely one of the diabetes-initiating self-antigens in mice [1] and humans [2–4]. We developed an oral antigen-specific vaccine using live attenuated *Salmonella* [5–7]. The *Salmonella*-based delivery system comprised PPI fused with effector (sseF) and expressed and secreted under control of the SPI2 promoter of the

Salmonella pathogenicity island 2-encoded type-3 secretion system (SPI2-T3SS) [8–10]. This was combined with the immunomodulators TGFβ and IL10 expressed and secreted under control of a cytomegalovirus (CMV) promoter [5]. The vaccine combined with low dose anti-CD3 mAb prevented and reversed diabetes in non-obese diabetic (NOD) mice [5–7, 11]. *Salmonella* genus belongs to *Enterobacteriaceae* (family), *Enterobacterales* (order), *Gammaproteobacteria* (class), and *Proteobacteria* (phylum) [12] and offers several advantages over the other methods of antigen delivery. *Salmonella* are taken up and internalized by gut antigen presenting cells (APCs) and remain alive in intracellular vacuoles where they pass proteins and genetic information to the host cells [13, 14]. Inside the cells, especially dendritic cells (DCs) and macrophages, the SPI2-T3SS passes proteins directly to the host cytoplasm. Self-antigens fused with SPI2 proteins that are passed directly into the cytosol of APCs can be processed and then presented to immune cells within the gut mucosa [8, 15–18]. Bypassing the expression of antigen in the intestinal lumen has the advantage of avoiding degradation and unwanted immune responses. *Salmonella* can influence host APCs by carrying mammalian expression plasmids and this feature was exploited to develop DNA vaccines [19, 20]. The same feature can be employed to carry tolerogenic cytokines that are directly expressed by the host cell, and hence can create a local immune-privileged microenvironment. Of clinical relevance, a *Salmonella* vaccine for typhoid fever is approved by the FDA.

Since the live *Salmonella* vaccine is orally administered it may alter the microbiota. The gastrointestinal tract microbiota consists of over a 1000 microbial species [21]. The microbiota exists in a state of homeostasis maintained by the action of gut-associated lymphoid tissues (GALTs) that generate regulatory T (Tregs) and effector T cells, B cells, and others. The cross talk between the microbiome and immune cells promotes tolerance. A balanced diverse microbiota was linked to improved digestion, metabolism, and an appropriate immune response to pathogens [22]. Microbiota imbalance, low diversity, and disproportionality are termed dysbiosis. Dysbiosis is associated with various diseases including inflammatory bowel, metabolic, and autoimmune diseases [22, 23].

Imbalance in the gut microbiota was linked to the development of T1D, type 2 diabetes (T2D), and obesity [24]. Moreover, lipopolysaccharide (LPS), as part of the outer membrane of Gram-negative bacteria, possibly derived from gut microbiota, may act as a molecular link between the gut microbiota, inflammation, and T1D. We showed that vaccination using *Salmonella*-based vaccine in combination with sub-therapeutic doses of anti-CD3 antibody reduced the development of diabetes and the severity of insulitis, preserved beta cell mass, and prevented glucose intolerance in mice [5, 6]. Furthermore, combination therapy was capable of reversing ongoing diabetes [7]. In both the prevention and reversal of diabetes, the vaccine significantly increased the number of Tregs in the spleen, mesenteric lymph nodes (MLN), Peyer's patches (PP) and pancreatic lymph nodes (PLN) [7].

Still, the oral *Salmonella*-based vaccine introduces live bacteria into the gut microbiota. This might have negative consequences on the native intestinal flora. Herein, we explored the effect of the vaccine on the composition and proportions of the gut microbiome and related metabolites in non-diabetic NOD mice.

Materials and methods

Salmonella vaccine

The attenuated strain of *Salmonella typhimurium* was employed for oral vaccination as described [5–7, 25]. Bacteria were cultured overnight in liquid growth media containing 50 μg/ml kanamycin or carbenicillin. The cultured bacteria were washed and suspended in 5% sodium bicarbonate for oral administration.

Animal experiments

Seven-week-old female NOD/ShiLtJ (NOD) mice (Jackson Laboratories, Bar Harbor, ME) were maintained under pathogen-free conditions and housed at the animal care facility at City of Hope National Medical Center. The study was approved by the Institutional Animal Care and Use Committee (IACUC# 18017). Eight-week-old mice were orally vaccinated with *Salmonella* containing plasmid for the expression of IL10 and TFGβ and *Salmonella* expressing autoantigen PPI in 200 ml of 5% sodium bicarbonate on days 0 and 7. Vaccinated animals were also treated with anti-CD3 mAb for five consecutive days (days -1 to 3). The control (vehicle) treatment was 200 ml of 5% sodium bicarbonate given orally. Stools were collected from vaccine-, and control- treated animals at pre, 3-, 7-, 14-, 30-day post-vaccination.

DNA extraction

DNA was extracted from feces using the QIAamp Fast DNA Stool Mini Kit (Qiagen, Hilden, Germany) [26]. The quality and purity of the isolated genomic DNA were confirmed by gel electrophoresis and quantitated with a Qubit2.0 fluorometer using the Qubit dsDNA HS Assay (Thermo Fisher Scientific, Waltham, MA). DNA samples were stored at -20˚C.

PCR amplification

Amplification of the 16S rRNA and 5.8S rRNA genes were performed using 16S-804 (5′– (TCC TACGGGAGGCAGCAGT–3′), 16S-515 (5′–GGA CTACCA GGG TATCTAATCCTG–3′), ITS1 (5′–TCC GTAGGTGAACCTGCGG–3′), and ITS4 (5′–TCC TCCGCTTATTGATATGC–3′) primers. For identification of fungi, the ITS region was amplified using ITS1 and ITS4 primers and the 16S rRNA gene (V3-V4) was used for bacteria. The PCR mixture was composed of Q5 High-Fidelity Master Mix (New England Biolabs) at a 1x concentration, along with a double volume of molecular grade water and 0.05 μL/mM of each primer. Undiluted DNA (1.5 mL) was added to each 50 mL reaction. Thermocycling conditions included an initial denaturation step (3 minutes at 98˚C), followed by 30 cycles of denaturation (10 seconds at 98˚C), annealing (10 seconds at 55˚C for the16S primers and 20 seconds at 58˚C for the ITS primers), extension (10 seconds at 72˚C), and a final extension step of 3 minutes at 72˚C. PCR products were separated using gel electrophoresis on 1.5% agarose gel.

Library preparation and sequencing

The amplicon library was cleaned and barcoded, followed by emulsion PCR using the Ion Torrent next-generation sequencing data analysis workflow (Thermo Fisher Scientific). Equal volumes of bacterial 16S rRNA and fungal ITS amplicons were pooled, cleaned with AMPure XP beads (Beckman Coulter, Brea, CA) to remove unused primers, and then exposed to endrepair enzyme for 20 minutes at room temperature. After an additional AMPure cleanup, ligation was performed at 25˚C for 30 minutes using Ion Torrent P1 and a unique barcoded "A" adaptor per pooled sample. After AMPure removal of residual adaptors, samples were concentrated to one quarter volume for 1 hour using a vacuum (Labconco, Kansas City, MO) under heat. All separate barcoded samples were then pooled in equal amounts (10 μL) and sizeselected for the anticipated 16S and ITS range (200 to 800 bp) using Pippin Prep (Sage Bioscience, Beverly, MA). The library was amplified for 7 cycles and quantitated on a StepOne qPCR instrument (Thermo Fisher Scientific) ahead of proper dilution to 300 pM going into the IonSphere templating reaction on the Ion Chef (Thermo Fisher Scientific). Library sequencing was completed on an Ion Torrent S5 sequencer (Thermo Fisher Scientific), and barcode-sorted samples were analyzed in our custom pipeline based on GreengenesV13_8 and Unite database

V7.2, designed for the taxonomic classification of 16S rRNA and ITS sequences, respectively. Sequencing reads were clustered into operational taxonomic units (3% distance), described by community metrics and taxonomically classified within the Qiime bioinformatics pipeline (ver. 1.9)

Metabolomics profiling

Metabolomic profiling was performed as published [27]. Feces (20 mg) was mixed with methanol: chloroform (1:1) and vortexed for 15 minutes. Samples were centrifuged at 10,000 RPM for 10 minutes and the filtrates were collected and dried using a rotatory evaporator (Buchi, Germany). The metabolite extracts were derivatized by adding 50 μL of *N*-trimethylsilyl-*N*-methyl trifluoroacetamide and trimethylchlorosilane (MSTFA + 1% TMS) mixture followed by incubation at 50˚C for 30 minutes prior to gas chromatography-mass spectrometry (GC-MS) analysis as described [28]. GC-MS measurements were carried out using an Agilent Model 7683 Autosampler, 6890 Gas Chromatograph and 5975 Inert Mass Selective Detector in the Electron Impact (EI) mode. EI energy was set to 70 eV. Separation was carried out on an Agilent HP5-MS column with dimensions 30 m x 250 μm x 0.25 μm. Ultra-High Purity Grade He (Airgas) was used as the carrier gas with the flow set to 0.8 mL/minute in constant flow mode. The initial oven temperature was set to 45˚C for 1 minute followed by a 30˚C/minute ramp to a final temperature of 300˚C, which was maintained for 3 minutes. A 3.2-minute solvent delay was used. The injector temperature was set at 220˚C. The MSD was set to scan the 40–1050 m/z range. Data collection and analysis were performed using MSD Enhanced Chemstation software (Agilent). Product spectra were identified by comparison of the measured fragmentation patterns to those found in the NIST 08 Mass Spectral Library.

Differential metabolite expression was calculated as the fold-change from day 0 (before vaccination) by employing Ingenuity Pathway Analysis (IPA, Qiagen, version 84978992) core analysis with metabolomics analysis by expression Log Ratio using default settings and no cutoffs. Assessment between timepoints was created using the comparison analysis tool in IPA. Analyzed pathway data was exported into CSV (comma-separated values) files and graphed in Prism.

Statistical analysis

A custom pipeline based on the Greengenes V13_8 database designed for the taxonomic classification of 16S rRNA sequences was employed. Downstream data analysis was performed using Qiime Platform (ver. 1.9) [29]. The Dunnett's multiple comparisons test and Dunn's multiple comparisons test (non-parametric) were used to analyze the differences in the percent abundance of gut microbiome within the same cohorts before and after vaccination (paired for longitudinal analysis). Bonferroni's and Mann-Whitney multiple comparisons tests were used to compare differences between vaccinated and vehicle-treated groups at different time points. Multiple paired t tests with adjusted p-values using the two-step Benjamini, Kreiger, and Yekutiele procedure were used to compare differences in post-vaccinated metabolite concentrations in animals on day 3, 7, 14, and 30 with pre-vaccinated levels. For all tests, a $p < 0.05$ was considered significant. Statistics were performed using Graphpad Prism software.

Results

Microbiota analysis

Fifty fecal samples were collected from vaccine- (n = 25) and control (vehicle)-treated NOD mice. The total number of bacteriome and mycobiome reads was 3.7 million. Annotated

sequences were used to study the microbial community using the phylotype approach. Sequences were assembled in operational taxonomic units (OTUs) at the lowest annotation level (genus). The relative abundance for each OTU was calculated. The resulting abundance matrix was used to calculate the community alfa diversity indexes. Relative abundances of bacterial and fungal phyla, genera, and species are represented in **S1** and **S2** **Figs**.

Effect of oral *Salmonella*-based combination therapy on gut bacteriome

To answer the question if the oral bacterial vaccine alters the gut bacterial community composition, the difference between vaccine- and vehicle-treated groups was assessed before and after vaccination on days 3, 7, 14, and 30 post-vaccination. The dynamics of the murine gut microbiota was studied at the levels of phylum and genus.

The murine gut microbiota was dominated by two bacterial phyla *Firmicutes* and *Bacteroidetes* that accounted for over ~ 95% of sequence reads at all time points (**S3A Fig**). The remaining diversity was attributed to *Verrucomicrobia*, *Tenericutes*, *Actinobacteria*, and *Proteobacteria* that accounted for ~ 4% of the remaining microbiota abundance. The phyla with abundance less than 1% were combined and designated "other" (**S3A Fig**). Longitudinal analysis of the fecal bacterial composition was conducted. At the phylum level, a significant decrease in *Firmicutes* on days 14 and 30 (p = 0.005) (**Fig 1B**) was observed for vaccine-treated mice, while no change in the *Firmicutes* was found in vehicle-treated mice (**Fig 1A**). *Bacteroidetes* was decreased on day 3 and significantly increased on day 30 (p = 0.009) (**Fig 1B**) in vaccine-treated mice, but not in vehicle-treated mice (**Fig 1A**). *Actinobacteria* was significantly increased in vaccine-treated mice on days 3, 7 and 30 (p = 0.01, p = 0.02, and p = 0.02, respectively) (**Fig 1B**), while a significant increase in *Actinobacteria* on day 30 (p = 0.028) was observed in vehicle-treated mice (**Fig 1A**). No change was detected in fecal *Protobacteria* in
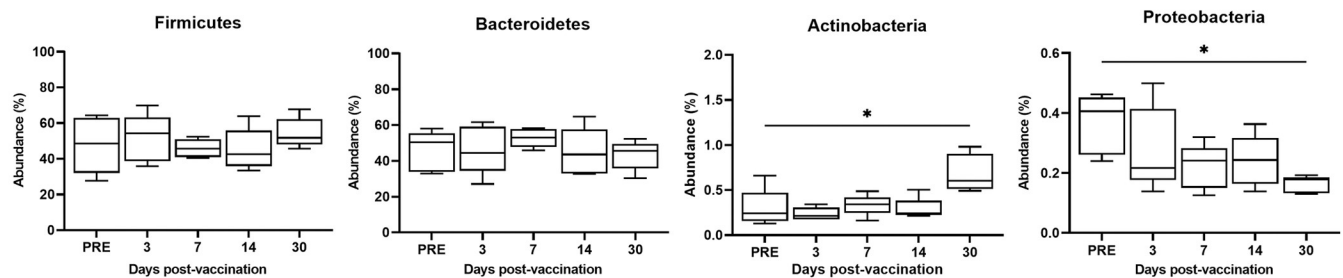
Fig 1. Boxplots of changes in abundance percentage of the gut bacteria at the phylum level within the same treated cohorts at different time points. The longitudinal analysis of 4 most abundant phyla including *Firmicutes*, *Bacteroidetes*, *Actinobacteria*, and *Proteobacteria* are shown within vehicle cohorts (A), and vaccine cohorts (B). Each time point represents the mean ± SD of 5 samples. The Dunnett's multiple comparisons test was used to analyze the significance between different time points using asterisks, *p < 0.05 and **p < 0.01.

vaccine-treated mice (**Fig 1B**), while in vehicle-treated mice a significant decrease in *Protobacteria* (p = 0.011) was noted (**Fig 1A**).

The genera levels of microbial dynamics are displayed in **S3B Fig**. Ten genera with abundance >1% are presented. The genera with abundance <1% were combined and designated "other" (**S3A Fig**). There genera dominated, *Lactobacillus*, *Oscillospira*, and *Akkermansia* accounting for ~ 75%. In longitudinal analysis, *Lactobacillus* was significantly increased on day 3 (p = 0.043) in vaccine-treated mice (**Fig 2B**) and significantly increased on days 7 (p = 0.007) and 30 (p = 0.034) in vehicle-treated mice (**Fig 2A**). The genus *Oscillospira* was significantly decreased on day 14 (p = 0.012) (**Fig 2B**) in vaccine-treated animals and little changed in vehicle-treated mice (**Fig 2A**). The genus *Ruminococcus* was significantly decreased on days 3 (p = 0.04) and 30 (p = 0.007) (**Fig 2B**) but decreased without significance in vehicle-treated mice (**Fig 2A**). No change in the abundance of *Akkermansia* in any of the mice was observed (**Fig 2**).

At the phylum level, changes over the 5 time points for the 6 most abundant fecal bacteria in vaccine-treated mice compared with the vehicle-treated mice are illustrated in **Fig 3.** The relative abundance of the phylum *Bacteroidetes* was significantly increased in the gut of vaccine-treated mice on day 30 (p = 0.024) and on day 7 (p = 0.03) for *Proteobacteria* compared with vehicle-treated mice (**Fig 3**). In contrast, the abundances in the bacterial phyla *Firmicutes* and *Actinobacteria* in vaccine-treated mice were significantly decreased on day 30 (p = 0.023, and p = 0.008) compared with vehicle-treated mice (**Fig 3**). No changes were observed in the relative abundance of the bacterial phyla *Verrucomicrobi*a and *Tenericutes* between vaccine- and vehicle-treated groups at any time points (**Fig 3**).

No significance changes occurred in the 6 most abundant fecal bacterial compositions at the genus level over any time points except a significant increase in the genus *Anaeroplasma* on day 7 (p = 0.008) and *Coprococcus* on day 14 (p = 0.03) in vaccine- compared with vehicle-treated mice (**Fig 4**).
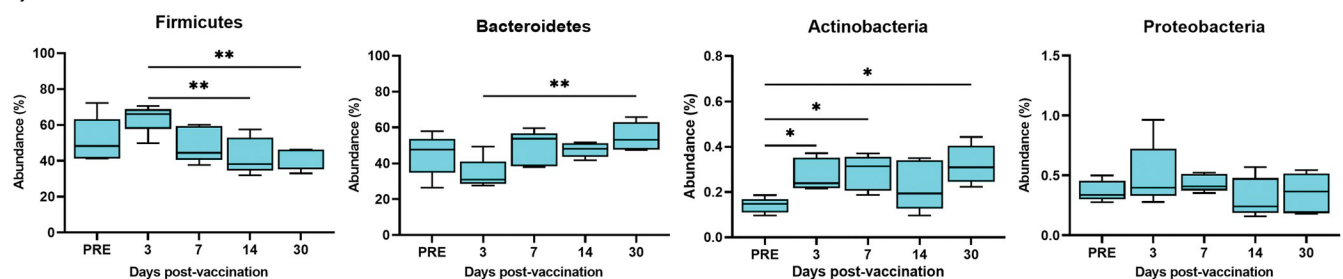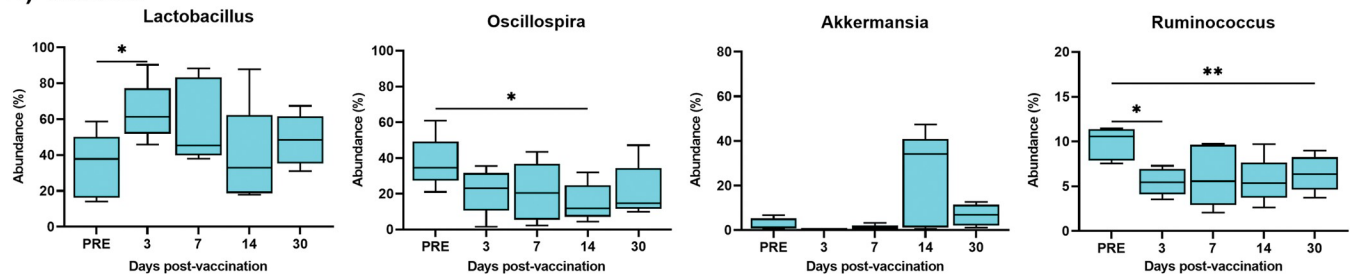

Fig 2. Boxplots of changes in abundance percentage of the gut bacteria at the genus level within the same treated cohorts at different time points. The longitudinal analysis of the 4 most abundant genera including *Lactobacillus*, *Oscillospira*, *Akkermansia*, and *Ruminococcus* are shown within vehicle cohorts (A), and vaccine cohorts (B). Each time point represents the mean ± SD of 5 samples. The Dunnett's multiple comparisons test was used to analyze the significance between different time points using asterisks, *p < 0.05, and **p<0.01.
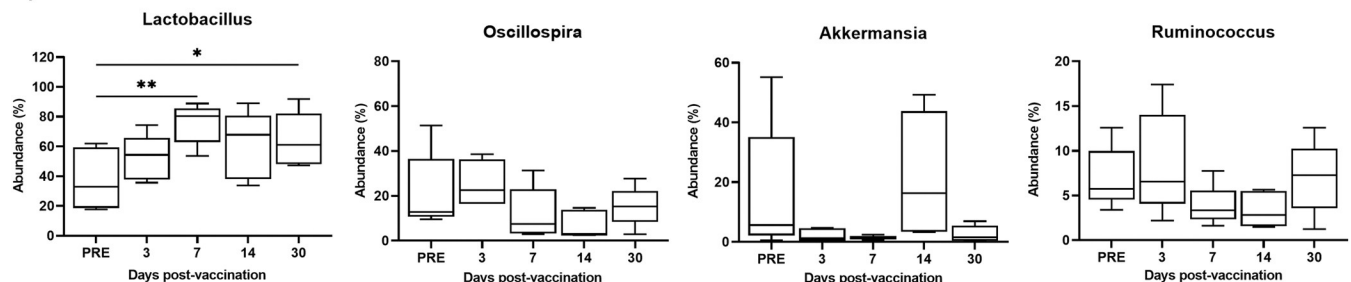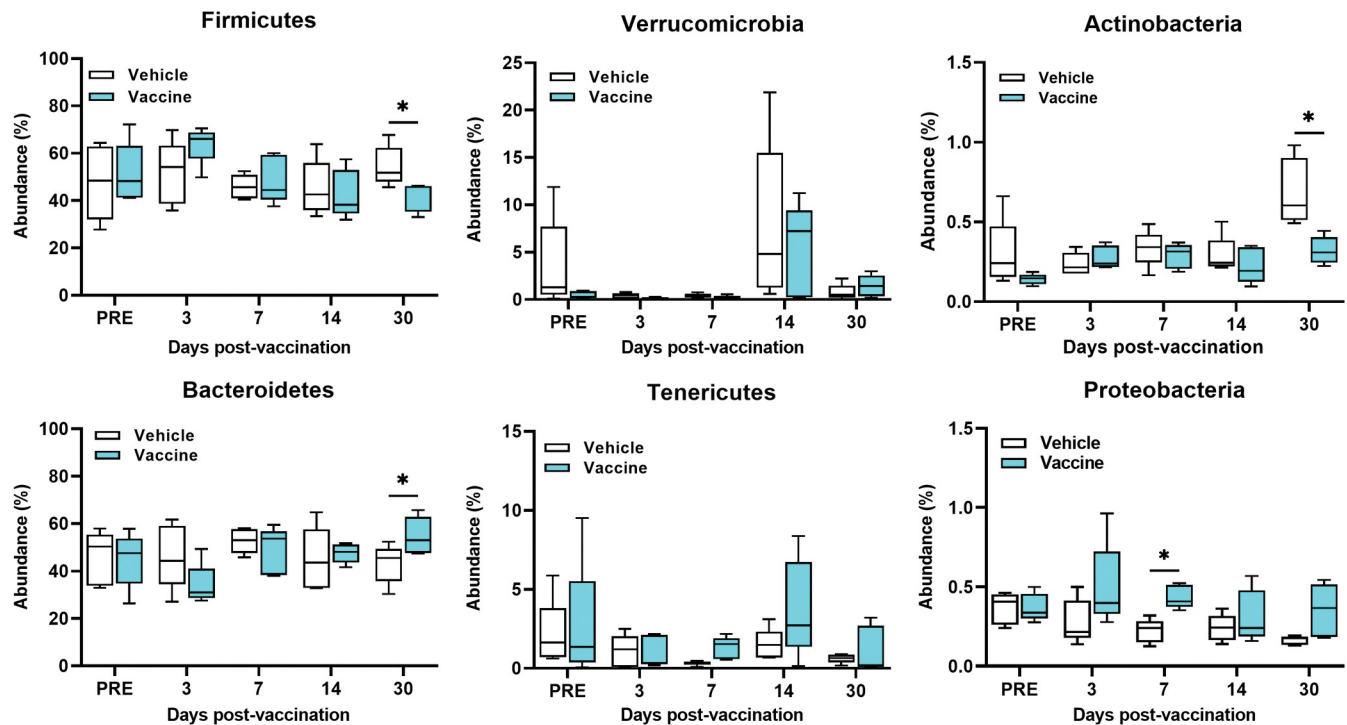
Fig 3. Boxplots of changes in abundance percentage of the gut bacteria at the phylum level. The 6 most abundant phylum including *Firmicutes*, *Bacteroidetes*, *Verrucomicrobia*, *Tenericutes*, *Actinobacteria*, and *Proteobacteria* are shown. Each time point represents the mean ± SD of 5 samples. Mann-Whitney with Holm-Sidak correction for multiple comparisons test was used to report significance between groups at each time point using asterisks, *p < 0.05.

There is a relation between *Salmonella* and phylum *Protobacteria*. Thus, a closer look into this was done. A significant increase in the phylum *Protobacteria* (relative abundance 0.5%) on day 7 (p = 0.029) occurred in vaccine-treated mice compared to vehicle-treated mice (**Fig 5**). The class *Gammaproteobacteria* (~0.3%) significantly increased on day 7 in vaccine- compared to vehicle-treated mice (p = 0.019) (**Fig 5**). Analyzing the class *Gammaproteobacteria* including families *Enterobacteriaceae* (0.3%) and *Pseudomonadaceae* (0.1%) revealed a relative abundance of fecal bacteria from *Enterobacteriaceae* with a significant increase noted in vaccine- compared to vehicle-treated on day 7 (p = 0.022) (**Fig 5**). Also, a significant increase in the relative abundance of the bacterial family *Pseudomonadaceae* was noted in vaccine- compared to vehicle-treated mice on days 7 (p = 0.008) and 30 (p = 0.008) (**Fig 5**).

Effect of oral *Salmonella*-based combination therapy on the gut mycobiome

The mouse gut mycobiome is dominated by the fungal phylum *Ascomycota* that accounted for over 99% of sequence reads (**S4A Fig**). The remaining detected phyla included *Basidiomycota*, *Zygomycota*, and *Glomeromycota*. No significant difference in the fecal fungal phyla between vehicle- and vaccine-treated animals at any time points (**S4A Fig**). No statistically significant differences in the 4 most abundant fecal fungi at the phylum level were noted across any time points between vaccine- and vehicle-treated mice (**S5A Fig**).

The composition of gut fungal genera of mouse feces was dominated by 4 genera. *Galactomyces*, *Eurotium*, *Candida*, and *Geotrichum* accounted for ~90% (**S4B Fig**). No statistically significant differences in the 4 most abundant fecal fungal genera were noted across all time points between vaccine- and vehicle-treated mice (**S5B Fig**).
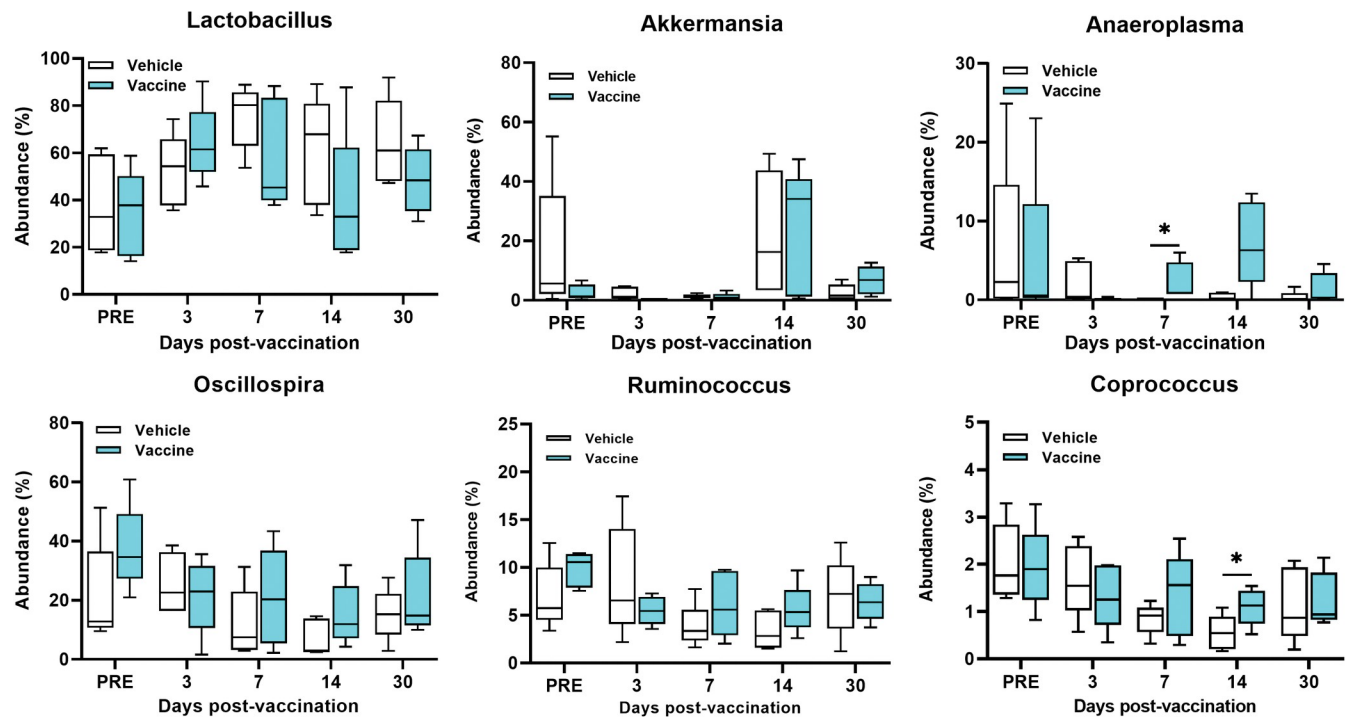
Fig 4. Boxplots of changes in the abundance percentage of the fecal bacteria at the genus level. The 6 most abundant genera including *Lactobacillus*, *Oscillospira*, *Akkermansia*, *Ruminococcus*, *Anaeriplasma*, and *Coprococcus* are shown. Each time point represents the mean ± SD of 5 samples. Mann-Whitney with Holm-Sidak correction for multiple comparisons test was used to report significance between groups at each time point using asterisks, *p < 0.05.

In summary, vaccination had no significant effect on gut microbiota composition immediately after initiation of treatment. The effects were noted at later times and were characterized by the increased abundance of the phylum *Bacteroidetes* and decreased abundance in *Firmicutes* and *Actinobacteria*.

Effects of an oral *Salmonella*-based combination therapy on the gut metabolome

Gut metabolic profiling was conducted on feces collected from NOD mice at pre- and post-vaccination days 3, 7, 14, and 30. Metabolomic profiling showed variation in the metabolites between samples (**Table 1**). The major metabolites identified were fatty acids such as palmitic
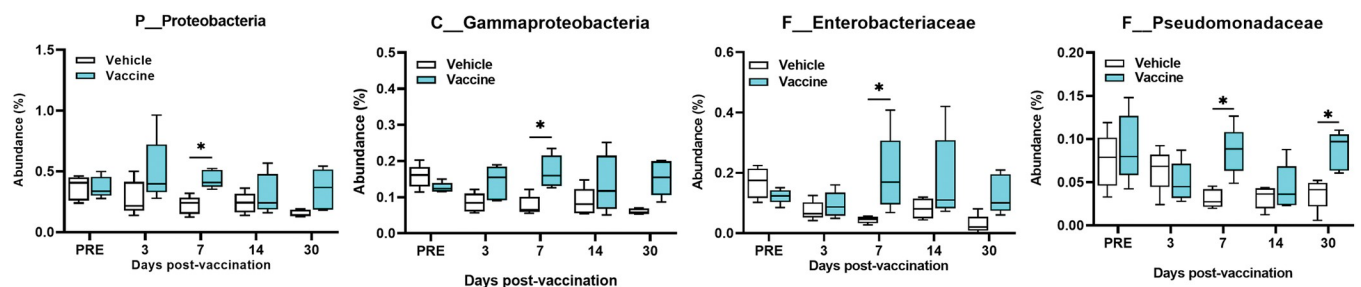
Fig 5. Boxplots of the changes in abundance percentage of the fecal selected phylum *Proteobacteria*. The percentage of class *Gammaproteobacteria*, families *Enterobacteriaceae* and *Pseudomonadaceae*, and genus *Pseudomonas*. Each time point represents the mean ±SD of 5 samples. Group of vaccinated mice compared with vehicle-treated at different time points. Mann-Whitney with Holm-Sidak correction for multiple comparisons test was used to report significance between groups at each time point using asterisks, *p < 0.05.

Table 1. Metabolites detected in the faces of NOD mice before and after vaccination using GC-MS.

Metabolite	Before vaccination		After vaccination												
	PRE		Day 3			Day 7			Day 14			Day 30		
	Average	±SD	Average	±SD	P #	Average	±SD	P #	Average	±SD	P #	Average	±SD	P #
Urea	ND	-	0.06	0.02	-	13.99	0.83	-	0.62	0.22	-	12.32	0.41	-
Uracil	0.87	0.03	0.34	0.08	0.011	0.24	0.06	<0.001	1.38	2.25	0.019	0.42	0.06	0.004
L-Leucine	0.37	0.12	0.26	0.11	0.454	0.56	0.07	0.225	0.59	0.16	0.553	0.44	0.10	0.062
L-Isoleucine	0.47	0.19	0.29	0.05	0.274	0.52	0.08	0.944	0.52	0.09	0.807	0.39	0.08	0.358
L-Tyrosine	0.43	0.07	0.37	0.01	0.238	0.52	0.11	0.325	0.66	0.13	0.110	0.45	0.05	0.748
L-Valine	0.38	0.05	0.19	0.07	0.101	0.43	0.09	0.309	0.55	0.09	0.052	0.42	0.04	0.165
Glycine	0.05	0.02	0.05	0.06	0.942	0.03	0.01	0.626	0.03	0.02	>0.999	0.02	0.01	0.374
DL-Alanine	1.415	0.22	0.10	0.08	0.117	0.83	0.24	0.245	1.24	0.17	0.449	1.07	0.18	0.509
L-Phenylalanine	0.36	0.07	ND	-	-	0.47	0.08	0.321	0.52	0.08	0.075	0.48	0.07	0.152
5-Oxoproline (Pyroglutamic acid)	0.99	0.15	0.46	0.11	0.078	0.51	0.07	0.266	0.79	0.13	0.218	0.43	0.06	0.013
Butanedioic acid (Succinic acid)	0.50	0.10	0.41	0.07	0.093	0.39	0.07	0.363	0.51	0.11	0.371	0.37	0.06	0.190
Oxalic acid	0.10	0.09	0.14	0.03	0.775	0.07	0.01	0.517	0.31	0.40	0.960	0.08	0.01	0.658
Glycolic acid (hydroacetic acid)	0.58	0.09	0.59	0.26	0.762	0.55	0.05	0.500	0.81	0.12	0.123	0.59	0.15	0.461
Butanoic acid (Ethyl acetic acid)	0.43	0.20	0.83	0.25	0.232	ND	-	-	0.82	0.04	0.088	0.14	0.04	0.350
5-Aminovaleric (Propylacetic) acid	0.32	0.24	0.52	0.11	0.106	1.20	0.27	0.034	0.88	0.14	0.046	0.69	0.17	0.087
3-Hydroxybutyric acid (BHBA)	0.52	0.01	0.25	0.15	0.439	0.06	0.01	0.175	0.09	0.01	0.475	ND	-	-
Lactic (2-Hydroxypropanoic) acid	2.72	0.58	7.18	0.89	0.004	2.80	0.55	0.299	4.68	0.71	0.060	2.54	0.59	0.735
3-Hydroxypropanoic (Ethylene lactic) acid	0.57	0.24	0.41	0.12	0.246	0.42	0.10	0.361	0.77	0.13	0.200	0.45	0.07	0.365
Hexadecanoic acid, ethyl ester (Palmitic) acid	0.66	0.04	0.79	0.16	0.656	0.51	0.11	0.395	0.96	0.12	0.076	0.94	0.18	0.334
Palmitic Acid	8.95	1.92	9.75	1.22	0.325	5.49	1.65	0.035	9.27	1.07	0.368	12.58	1.22	0.161
Myristic acid	1.30	0.33	1.00	0.25	0.602	ND	-	-	0.71	0.12	0.043	0.69	0.19	0.024
Octanoic acid (Caprylic acid)	0.24	0.06	0.15	0.04	0.075	ND	-	-	0.30	0.14	0.462	0.22	0.06	0.960
Pentadecanoic acid	0.58	0.13	0.81	0.19	0.238	0.72	0.04	0.097	0.67	0.16	0.449	0.78	0.16	0.085
Stearic acid	1.66	0.49	2.12	0.46	0.086	1.24	0.33	0.299	1.81	0.43	0.993	2.37	0.44	0.025
Heptadecanoic (Margaric) acid	0.51	0.31	0.280	0.06	0.206	0.20	0.04	0.166	0.24	0.08	0.256	0.29	0.06	0.258
1-Tetradecanol	0.45	0.27	0.683	0.09	0.162	0.30	0.12	0.889	0.50	0.06	0.747	0.50	0.06	0.693
10-Undecynoic acid	0.88	0.11	0.663	0.15	0.342	0.58	0.06	0.038	0.10	0.01	0.042	0.66	0.09	0.190
Oleic Acid	1.10	0.07	0.170	0.06	0.007	1.20	0.56	0.214	1.11	0.13	0.959	0.54	0.04	0.005
α -Linolenic acid	ND	-	1.070	0.06		ND	-	-	ND	-	-	0.92	0.42	-
9,12-Octadecadienoic (Linoleic) acid	4.82	0.68	4.880	0.46	0.931	3.14	0.24	0.268	2.24	0.66	0.079	5.12	0.75	0.620
Azelaic acid	0.49	0.01	0.342	0.11	0.006	0.35	0.09	0.135	0.74	0.12	0.105	0.44	0.08	0.605
Ethanolamine	2.00	0.34	1.125	0.21	0.112	0.65	0.09	0.007	ND	-	-	0.81	0.11	0.011
4-Hydroxybenzeneacetic acid	0.64	0.17	0.533	0.06	0.498	0.547	0.09	0.336	0.74	0.26	0.823	0.56	0.07	0.497
3-(3-Hydroxyphenyl) propanoic acid	1.57	0.46	3.203	0.13	0.025	1.51	0.31	0.934	2.39	0.97	0.244	2.33	0.80	0.163
Phloretic (3-(4-Hydroxyphenyl) propanoic) acid	0.34	0.02	0.587	0.15	0.330	0.22	0.05	0.170	0.55	0.10	0.085	0.37	0.09	0.747
Eicosane	0.43	0.11	0.964	0.14	<0.001	0.84	0.06	<0.001	1.98	0.63	0.005	0.59	0.07	0.001
Heptadecane	0.43	0.09	0.246	0.04	0.028	0.22	0.06	0.068	0.62	0.11	0.078	0.16	0.03	0.011
Cholesterol	0.36	0.04	0.630	0.08	0.061	0.50	0.06	0.088	0.56	0.11	0.154	0.58	0.07	0.022
Cholestan-3-ol (Coprostanol)	0.13	0.02	0.158	0.04	0.020	0.13	0.01	0.580	0.10	0.06	0.625	0.15	0.03	0.011
24-Ethyl-.delta.(22)-Coprostenol	0.04	0.01	0.080	0.01	0.060	0.05	0.01	0.423	0.24	0.21	0.235	0.08	0.02	0.082
Stigmastanol	0.24	0.06	0.166	0.04	0.067	0.15	0.01	0.019	0.25	0.02	0.547	0.23	0.03	0.724
Campesterol	0.24	0.05	0.182	0.05	0.123	0.19	0.02	0.242	0.30	0.05	0.218	0.26	0.03	0.949
Stigmasterol	0.12	0.04	0.095	0.01	0.369	0.07	0.02	0.344	0.15	0.03	0.286	0.08	0.01	0.306
β.-Sitosterol	0.10	0.02	0.120	0.01	0.074	0.09	0.02	0.500	0.12	0.01	0.321	0.09	0.01	0.184

(Continued)

Table 1. (Continued)

Metabolite	Before vaccination		After vaccination											
	PRE		Day 3			Day 7			Day 14			Day 30		
	Average	±SD	Average	±SD	P #	Average	±SD	P #	Average	±SD	P #	Average	±SD	P #
D-Ribose	0.65	0.20	0.540	0.21	**0.568**	ND	-	-	ND	-	-	0.76	0.04	**0.933**
L-Rhamnose	0.49	0.42	1.020	0.06	**0.012**	ND	-	-	0.23	0.01	**0.431**	0.80	0.34	**0.298**
Xylose	0.21	0.03	0.243	0.05	**0.529**	0.18	0.09	**0.795**	0.25	0.04	**0.156**	0.23	0.05	**0.423**
β- D-(+)-Xylopyranose	0.94	0.57	0.958	0.08	**0.951**	ND	-	-	0.65	0.08	**0.503**	0.90	0.10	**0.920**
D-(+)-Talofuranose	0.29	0.06	0.275	0.12	**0.971**	0.27	0.05	**0.950**	0.26	0.06	**0.701**	0.29	0.05	**0.669**
Levoglucosan	1.68	0.65	0.267	0.04	**0.184**	0.88	0.04	**0.315**	0.32	0.08	**0.216**	0.16	0.04	**0.170**
Glucopyranose	1.00	0.09	0.724	0.17	**0.082**	0.86	0.12	**0.012**	0.44	0.07	**0.008**	0.76	0.18	**0.056**
Methyl α.-D-glucofuranoside	2.14	0.55	2.475	0.47	**0.122**	1.16	0.26	**0.007**	1.29	0.30	**0.023**	1.11	0.41	**0.010**
N-Acetyl-D-galactosamine	0.30	0.09	0.437	0.05	**0.267**	0.31	0.05	**0.858**	0.60	0.10	**0.050**	0.26	0.03	**0.203**
Glyceric acid	0.81	0.10	1.026	0.28	**0.454**	0.76	0.34	**0.907**	0.97	0.50	**0.482**	1.18	0.44	**0.041**
Glycerol	0.85	0.22	1.047	0.33	**0.590**	4.84	1.86	**0.110**	ND	-	-	2.29	0.67	**0.022**
1-Monooleoylglycerol	0.26	0.09	ND	-	-	0.16	0.05	**0.336**	0.15	0.07	**0.089**	ND	-	-
Glycerol monostearate	1.78	0.28	1.880	1.16	**0.928**	1.24	0.10	**0.006**	1.59	0.47	**0.829**	1.61	0.36	**0.351**
1-Monopalmitin (Glyceryl palmitate)	0.40	0.06	0.610	0.06	**0.088**	0.21	0.05	**0.004**	0.35	0.05	**0.396**	0.38	0.07	**0.714**
1,3-Propanediol	0.15	0.05	0.150	0.03	**0.500**	0.09	0.02	**0.053**	0.02	0.01	**0.025**	0.10	0.03	**0.597**
2,6-Bis (tert-butyl) phenol	2.59	0.40	1.616	0.27	**0.017**	ND	-	-	1.63	0.59	**0.132**	1.72	0.30	**0.028**

The amount represents the relative percentage of a metabolite in relation to total metabolites detected in the fecal pellet for 5 mice before and on days 3, 7, 14, and 30 post-vaccination ± SD. The statistical significance was calculated using multiple paired *t* test with Benjamini, Kreiger, and Yekutiele corrected significance level indicated (p value < 0.05). Red p value means significant increase and blue p value means significant decrease in comparison to the pre-treated group.

acid, myristic acid, oleic acid, stearic acid, 6-octadecenoic acid (petroselaidic acid), α-linolenic acid, 1,4-butanediol, 1-pentadecanol, butanoic acid, pentadecanoic acid, and heptadecanoic acid; amino acids such as L-leucine, L-isoleucine, L-valine, L-tyrosine, L-alanine, and phenyl-alanine; and sugars such as β-D-(+)-xylopyranose, glycerol, L-rhamnose, D-ribose, α-d-gluco-pyranoside, in addition to urea, and 3,5-dihydroxybenzoic acid (**Table 1**).

Some of these metabolites showed specific patterns following vaccination. L-leucine was significantly decreased in the feces following vaccination on days 3 and 7 and then significantly increased on day 14 and dropped again on day 30 while L-5-oxoproline (pyroglutamic acid) was decreased after vaccination and more so on day 30. Other amino acids including L-isoleu-cinem, L-valine, L-alanine, L-tyrosine, glycine, and phenylalanine were varied (**Fig 6**).

The short-chain fatty acids (SCFA) derivative 5-aminovaleric acid (propylacetic acid) was significantly increased on days 7 and 14 while L-lactic acid (2-hydroxypropanoic acid) was significantly increased (day 3) after vaccination then returned to normal. No effect was noted on glycolic acid (hydracetic acid) and 3-hydroxypropanoic (ethylene lactic) acid while 3-hydroxybutyric acid was decreased after vaccination (**Fig 6**).

Saturated fatty acids (SFA) including myristic acid on days 14 and 30 and palmitic acid at day 7 were significantly decreased in feces following vaccination. On the other hand, stearic acid was significantly increased on day 30 in feces following vaccination while other SFA such as hexadecanoic acid ethyl ester (palmitic acid), pentadecanoic acid, and heptadecanoic acid (margaric acid) varied but without significant changes (**Fig 6**).

Unsaturated fatty acids (UFA) such as 10-undecynoic acid (at days 7 and 14) and oleic acid (on days 3 and 30) were significantly decreased following vaccination while α-linolenic acid was detected only on days 3 and 30 following vaccination (**Fig 6**). Interestingly, azelaic acid as

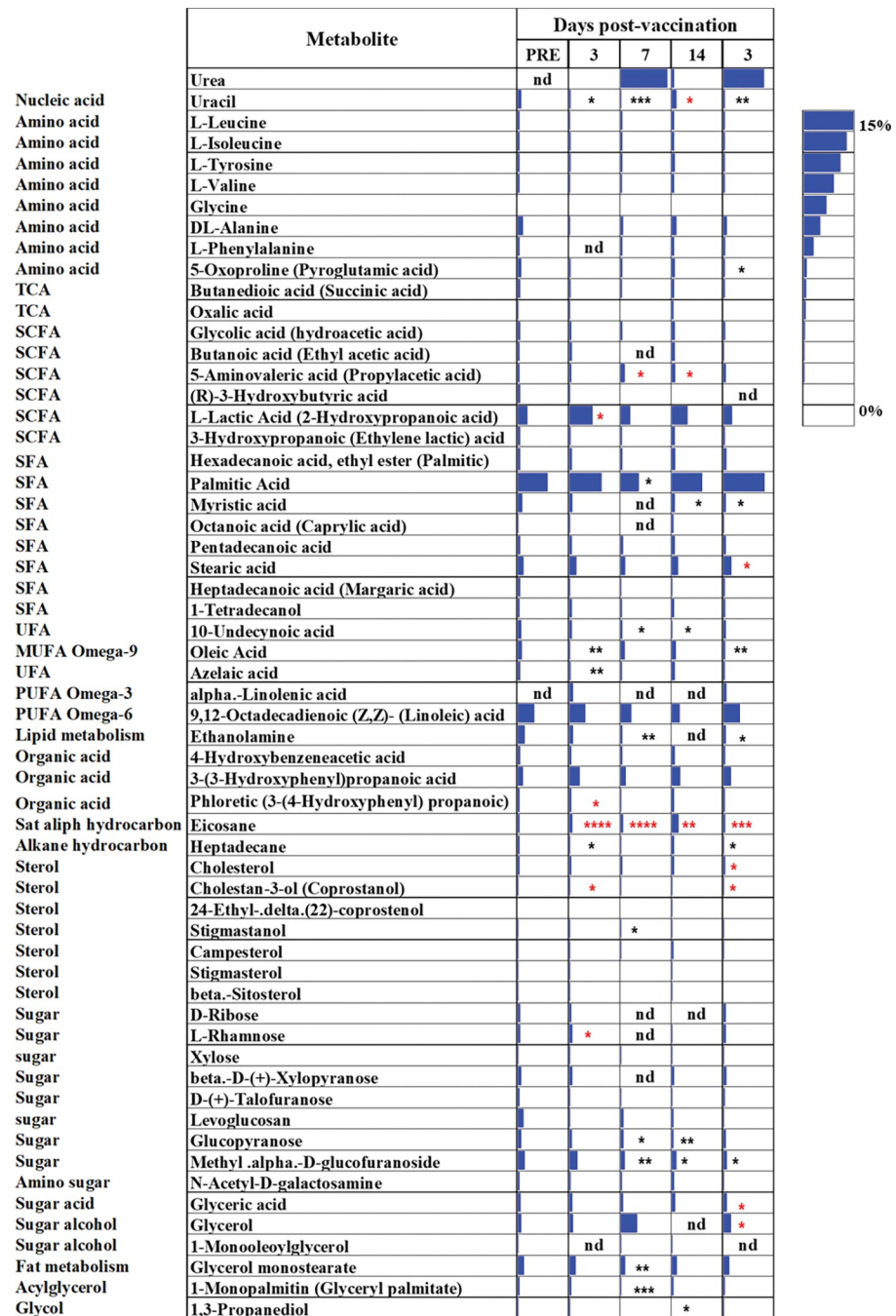| Category	Metabolite	PRE	3	7	14	3
	Urea	nd				
Nucleic acid	Uracil		*	***	* (red)	**
Amino acid	L-Leucine					
Amino acid	L-Isoleucine					
Amino acid	L-Tyrosine					
Amino acid	L-Valine					
Amino acid	Glycine					
Amino acid	DL-Alanine					
Amino acid	L-Phenylalanine		nd			
Amino acid	5-Oxoproline (Pyroglutamic acid)					*
TCA	Butanedioic acid (Succinic acid)					
TCA	Oxalic acid					
SCFA	Glycolic acid (hydroacetic acid)					
SCFA	Butanoic acid (Ethyl acetic acid)			nd		
SCFA	5-Aminovaleric acid (Propylacetic acid)			* (red)	* (red)	
SCFA	(R)-3-Hydroxybutyric acid					nd
SCFA	L-Lactic Acid (2-Hydroxypropanoic acid)		* (red)			
SCFA	3-Hydroxypropanoic (Ethylene lactic) acid					
SFA	Hexadecanoic acid, ethyl ester (Palmitic)					
SFA	Palmitic Acid			*		
SFA	Myristic acid			nd	*	*
SFA	Octanoic acid (Caprylic acid)			nd		
SFA	Pentadecanoic acid					
SFA	Stearic acid					* (red)
SFA	Heptadecanoic acid (Margaric acid)					
SFA	1-Tetradecanol					
UFA	10-Undecynoic acid			*	*	
MUFA Omega-9	Oleic Acid		**			**
UFA	Azelaic acid		**			
PUFA Omega-3	alpha.-Linolenic acid	nd		nd	nd	
PUFA Omega-6	9,12-Octadecadienoic (Z,Z)- (Linoleic) acid					
Lipid metabolism	Ethanolamine			**	nd	*
Organic acid	4-Hydroxybenzeneacetic acid					
Organic acid	3-(3-Hydroxyphenyl)propanoic acid					
Organic acid	Phloretic (3-(4-Hydroxyphenyl) propanoic)		* (red)			
Sat aliph hydrocarbon	Eicosane		**** (red)	**** (red)	** (red)	*** (red)
Alkane hydrocarbon	Heptadecane		*			*
Sterol	Cholesterol					* (red)
Sterol	Cholestan-3-ol (Coprostanol)		* (red)			* (red)
Sterol	24-Ethyl-.delta.(22)-coprostenol					
Sterol	Stigmastanol			*		
Sterol	Campesterol					
Sterol	Stigmasterol					
Sterol	beta.-Sitosterol					
Sugar	D-Ribose			nd	nd	
Sugar	L-Rhamnose		* (red)	nd		
sugar	Xylose					
Sugar	beta.-D-(+)-Xylopyranose			nd		
Sugar	D-(+)-Talofuranose					
sugar	Levoglucosan					
Sugar	Glucopyranose			*	**	
Sugar	Methyl .alpha.-D-glucofuranoside			**	*	*
Amino sugar	N-Acetyl-D-galactosamine					
Sugar acid	Glyceric acid					* (red)
Sugar alcohol	Glycerol				nd	* (red)
Sugar alcohol	1-Monooleoylglycerol		nd			nd
Fat metabolism	Glycerol monostearate			**		
Acylglycerol	1-Monopalmitin (Glyceryl palmitate)			***		
Glycol	1,3-Propanediol				*	

Legend bar: 15% / 0%

Fig 6. Heatmap comparing the metabolites extracted from feces of NOD mice at different times point pre- and post-vaccination using GC-MS. Feces collected from mice before and after vaccination at days 3, 7, 14, and 30. The amount represents the relative percentage of a metabolite in relation to total metabolites detected in a fecal pellet. Metabolite average relative percentages of 5 mice at each time point are displayed as blue bars. The statistical significance was calculated using multiple paired *t* test with Benjamini, Kreiger, and Yekutiele corrected significance level indicated asterisks ($*p < 0.05$, $**p<0.01$, $***p<0.005$, $****p<0.001$). Red asterisks mean a significant increase and black asterisks mean a significant decrease in comparison to the pre-treated group. SCFA (short-chine fatty acid); SFA (saturated fatty acid); UFA (unsaturated fatty acid); MUFA (monounsaturated fatty acid); PUFA (polyunsaturated fatty acid); TCA (tricarboxylic acid cycle); nd (not detected).

a product of oleic acid was significantly decreased in the feces on day 3 following vaccinations while no changes were noted in the 9,12-octadecadienoic acid (linoleic acid) (**Fig 6**).

Other acids such as 3-(3-hydroxyphenyl) propanoic acid (3-hydroxycinnamic acid) was significantly increased in the feces at day 3 following vaccination and then returned to normal levels on day 30. Other metabolites such as phloretic acid (3-(4-hydroxyphenyl) propanoic acid) and 4-hydroxybenzeneacetic acid were not changed in the feces after vaccination while ethanolamine was significantly decreased on days 7 and 30 after vaccination. Eicosane, a saturated hydrocarbon, was significantly increased after vaccination while heptadecane was significantly decreased (**Fig 6**).

Sugar metabolites including levoglucosan (on day 30), and glucopyranose, and methyl alpha-D-glucofuranoside were significantly decreased in the feces following the vaccination, while D-ribose, D- (+)-talofuranose, xylose, beta-D-(+)-xylopyranose and N-acetyl-D-galactosamine did not change in the feces after vaccination. L-rhamnose was significantly increased on day 7 in the feces after vaccination (**Fig 6**).

Glycerol monostearate (2-monostearin) and glyceryl palmitate (1-monopalmitin) were significantly decreased on day 7 following vaccination and returned to normal on day 14, and 1,3-propanediol was significantly decreased on day 14. Glycerol and glyceric acid were increased after vaccination and become significantly increased on day 30 (**Fig 6**).

Steroid metabolites detected in feces such as cholesterol (on day 30) and cholestane-3-ol (coprostanol) were significantly increased on days 3 and 30 after vaccination while stigmastanol was significantly decreased on day 14. Others such as stigmasterol, β-sitosterol, and campesterol 24-ethyl-delta (22)-coprostenol were not changed after vaccination (**Fig 6**).

Fecal metabolites such as succinic acid (butanedioic acid) and oxalic acid were not changed following vaccination (**Fig 6**). Urea was detected in the feces of the animal on day 3 then sharply increased on day 7 followed by a decrease on day 14 and then a final increase on day 30 post-vaccination while uracil (a nucleic acid) was significantly decreased following vaccination (**Fig 6**).

To understand the significance of the metabolomic changes, we utilized Ingenuity Pathway Analysis (IPA). Metabolite data (**Table 1**) were entered as fold change in relation to data collected from day 0 (pre-vaccine). The predicted disease and functions pathways identified within molecular functions showed an overall decrease in the ATP production, as seen in the pathways 'Release of ATP', 'Concentration of ATP', and 'Synthesis of ATP' (**Fig 7A**). Upregulated pathways involved cell death (Apoptosis, Necrosis) on days 3, 14, and 30 post-vaccines but these decreased on day 7 (**S6A Fig**). A potential activation of immune cell functions (Endocytosis by eukaryotic cells, Engulfment of cells) was noticed with an increased activity at all days post vaccination. Other pathways showed a trending decrease in 'Release of reactive oxygen species' and 'Generation of superoxide' or a trending increase in 'Synthesis of carbohydrate', 'Concentration of cholesterol', 'Synthesis of D-glucose', and 'Biosynthesis of hydrogen peroxide' (**S6A Fig**).

Further analysis of immune-focused diseases and functions was performed (**Fig 7B**). The 'Activation of leukocytes' was increased on days 3, 7, and 14 post-vaccines but decreased on day 30. Other pathways, such as 'Inflammatory response', 'Activation of phagocytes', 'Activation of macrophages', 'Activation of myeloid cells' and 'Proliferation of CD4+ T-lymphocytes' were increased on all days except day 7. Finally, in the first 14 days, 'Leukopoiesis' (formation of white blood cells) and 'Inflammation of organ' were decreased. This suggests a vaccine-associated activation of the immune system (**S6B Fig**).

The metabolite data were processed to determine if the changes of global regulators could be predicted. Using IPA Upstream Regulator Analysis, we identified proteins that are predicted to be activated or inhibited (**Fig 7C**). Of note, the anti-inflammatory cytokine IL-37 [30] is predicted to be activated days 3, 7, and 30 post-vaccination. Also, different regulators of mitochondria and metabolism were predicted to be upregulated on day 7 including NAD(P) transhydrogenase (NNT: mitochondria redox) [31], lipid-sensing peroxisome proliferator-
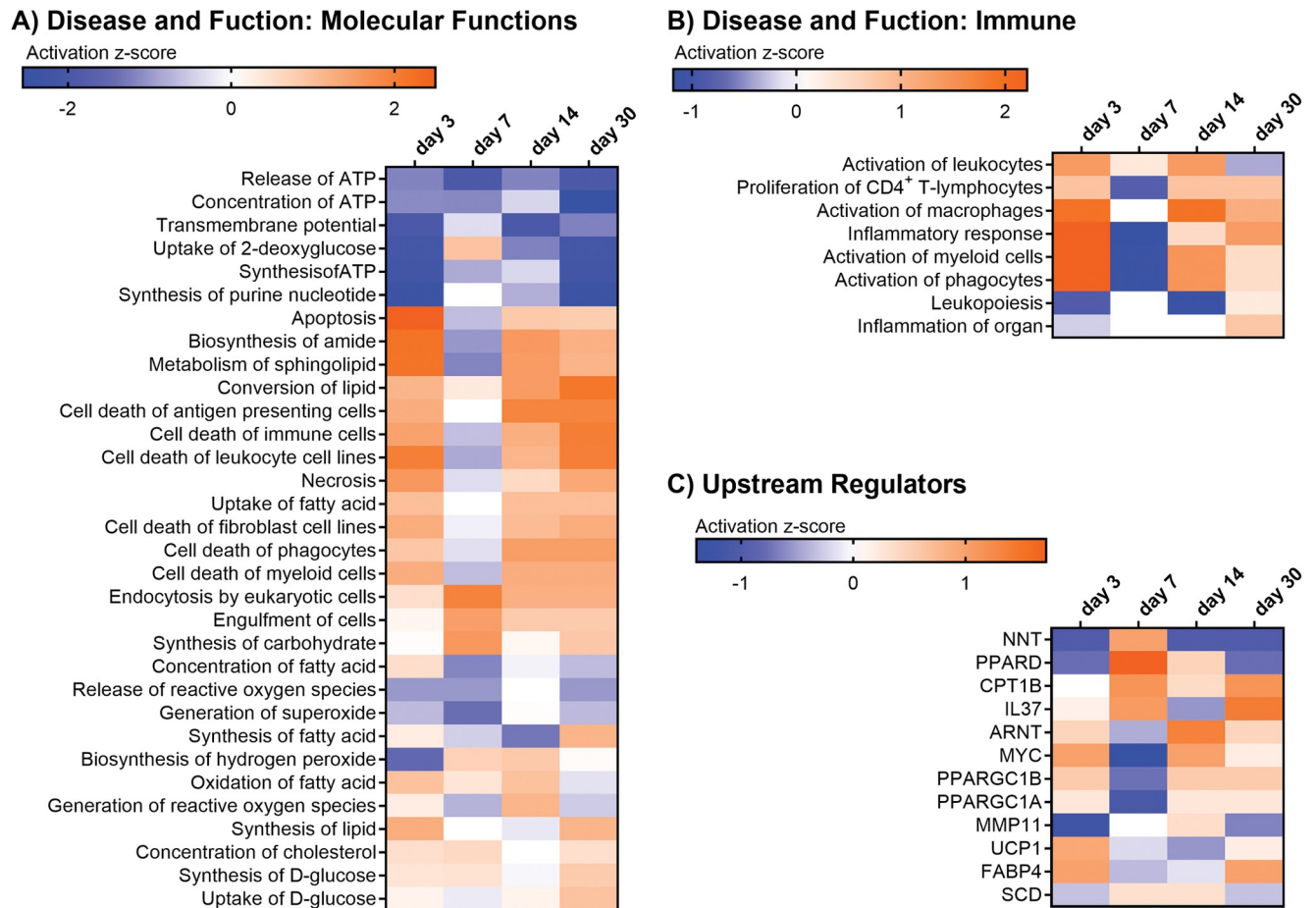
A) Disease and Fuction: Molecular Functions

B) Disease and Fuction: Immune

C) Upstream Regulators

Fig 7. IPA pathway analysis of fecal metabolites pre- and post-vaccination. Identified Disease and Functions pathways for Molecular Functions (A) and Immune (B) pathways are shown to be significantly changed on days 3, 7, 14, and 30 post-vaccines. A z-score above 1.3 indicates significant upregulation (orange) when compared to day 0 (pre-vaccine). Conversely, a z-score below -1.3 indicates significant down regulation (blue). Upstream Regulators (C) identifies predicted global regulators that have been activated (orange) or inhibited (blue) which may explain the observed changes in metabolites.

https://doi.org/10.1371/journal.pone.0285905.g007

activated receptor delta (PPARD) [32], and long-chain fatty acid transport carnitine palmitoyl-transferase I (CPT1B) [33]. While both NNT and PPARD were downregulated on days 3 and 30. Other transcriptomic co-factors and regulators, such as ARNT (aryl hydrocarbon receptor nuclear translocator) [34], MYC [35] and PPARGC1 (Peroxisome proliferator-activated receptor gamma coactivator 1) [36], were predicted to be upregulated on days 3, 14 and 30 post-vaccination. Uncoupling protein 1 (UCP1) [37] growth factor and fatty acid binding protein 4 (FABP4) [38] were upregulated on days 3 and 30 but downregulated on days 7 and 14 post-vaccination. Matrix metalloproteinase 11 (MMP11) [39], an inflammatory mediator, and stearoyl-CoA desaturase (SCD) [40], an enzyme that participates in the synthesis of UFA from SFA, were downregulated on days 3 and 30 post-vaccination (**S6C Fig**). Overall, this analysis indicated a significant change in metabolism, inflammation and proliferation following vaccine administration.

Discussion

An oral antigen-specific vaccine using live attenuated *Salmonella* prevented and reversed T1D in NOD mice [5–7]. To better understand possible effects of the vaccine, changes in the

composition of the gut microbiota were determined at different time points following vaccination. This is important because the microbiota can protect the host against microbial pathogens [41] while effects of *Salmonella* infection on the gut microbiota may lead to inflammation that favors the growth of pathogens [42, 43]. And while the *Salmonella* strain employed in the vaccine was attenuated, it still retained some infectious capacity.

Changes in the gut microbiota were implicated in altering diabetes susceptibility in NOD mice [44, 45]. Related to this, changes in the gut microbiome were seen between healthy and diabetic individuals mimicking to an extent data from NOD mice [46]. In this study, we compared the gut microbiome in vaccine- and vehicle-treated prediabetic mice. We found no changes in the composition of gut microbiota on the phylum level after vaccine administration except for a decrease in *Firmicutes*, and *Actinobacteria* on day 30 and increase in *Bacteroidetes* on day 30. Furthermore, no changes in the composition of bacteria genera between vaccine- and vehicle-treated mice were noted at any time points except an increase of *Anaeroplasma* and *Corprococcus* on days 7 and 14, respectively. Our vaccine combination caused an increase in the gut phylum *Proteobacteria*, the class *Gammaproteobacteria*, and the families *Pseudomonadaceae*, and *Enterobacteriaceae*. *Salmonella* genus belongs to *Enterobacteriaceae* (family), *Gammaproteobacteria* (class), and *Proteobacteria* (phylum) [12]. This could be important for the changes seen after vaccination. Overall, the data indicate that administration of the *Salmonella*-based vaccine altered the balance of the gut microbiota in prediabetic NOD mice. However, the modest changes noted before and after treatment within the same treatment-group (either vaccine group or vehicle group) were likely due to other factors such as type of food, handling, temperature, and age. The slight increase in family *Pseudomonadacea* may be attributed to an imbalanced gastrointestinal environment due to temporary changes in the composition of the gut microbiome [47].

Studying the changes in the composition of gut microbiota at short (7–14 days post vaccination) and longer times (30 days post-vaccination) reflects the expected lifecycle of the vaccine. Short term, there was an increase in only a few taxa by the vaccine, suggesting a successful infection and proliferation of the vaccine within the GALT. At day 30, the composition of microbiota mostly returned to its pre-vaccinated state except for an increase in the *Bacteroidetes* phylum and decrease in the *Firmicutes* and *Actinobacteria*. Narratively, this aligns with our data on the approximate 3-week clearance time of the vaccine. This suggests that the microbiota may have assumed a more tolerant state. When the vaccine successfully infiltrated the GALT, Treg abundance was increased throughout several lymphatic tissues especially on day 30 post-vaccination and this was associated with less beta cell injury [6, 7]. Of some possible relevance, gut *Bacteroidetes* were associated with increased Tregs [22]. Based on our data, we postulate that the microbiota responded to the vaccine and participated in immune regulation and induction of tolerance by increasing Tregs and regulatory cytokines and decreasing inflammatory cytokines [6, 7]. The intestinal epithelium plays an important role as a filter that translocates water, nutrients, and bio-reactive compounds from the intestine to the circulation [48]. Inflammation can increase the intestinal permeability to permit antigens to induce autoimmune response and promote the development of diabetes [49, 50].

In this study, the metabolic profiling of the vaccine-treated animals was determined and identified. Of the 60 identified metabolites, almost a third was associated with diabetes. The rest of the common metabolites were associated with digestion and were expected based on the diet of the mice. For example, amino acids (AA) including glycine and alanine are associated with glucose metabolism through promoting insulin secretion [51, 52]. Furthermore, elevated levels of valine, isoleucine, leucine, tyrosine, and phenylalanine are correlated with insulin intolerance and secretion suppression [53, 54]. Throughout, the levels of most of AAs showed high variance from day to day. However, by day 30 most of the AAs returned to pre-

vaccination levels. Of note, multiple predicted Upstream Regulators were up or down regulated based on the combination of changes in amino acid concentrations (**Fig 7C**). For example, CPT1B was predicted to be upregulated because of the increase in leucine and valine, and the decrease in alanine, glycine, and uracil (**S6C Fig**). When MMP11 is active, it could up-regulate amino acids such as alanine, glycine, isoleucine, tyrosine, phenylalanine, and ethanolamine. Also, due to the combined effects of alanine and glycine, in association with butyric acid and succinic acid, the anti-inflammatory protein IL37 is predicted to be activated on all days observed except day 14 (**S6C Fig**).

Lactate is produced by gut bacteria under anaerobic conditions and is metabolized in the colon by lactate-utilizing bacteria to produce beneficial short-chain fatty acids (SCFAs) including butyrate and propionate. Lactate metabolites play an important role in the stability of the gut microbiome [55]. SCFA metabolites generated by gut microbiota exert systemic anti-inflammatory effects through involvement in the production of immunoglobulin A and immunosuppressive cytokines [56]. These SCFAs may have an effect on metabolic and immune response, and inflammatory disease [57, 58]. For example, changes in the 'Biosynthesis of hydrogen peroxidase are due, in part, to the changes in butyric and succinic acids (**S6A Fig**). SCFAs such as acetate and propionate can influence insulin sensitivity and glucose tolerance via glycemic-mediated response. Propionate can decrease the fasting blood glucose, reduce gluconeogenesis, promote the utilization of glucose, and elevate glucagon-like peptide [59].

Butyrate maintains the integrity of the gut epithelium by inducing mucin synthesis [57]. NOD mice had lower abundance of SCFAs, especially butyrate, when compared to non-diabetic mice [60]. Significant elevations in 3-hydroxybutyric acid (β-hydroxybutyric acid, BHBA) is an indicator of diabetic ketoacidosis in T1D [61, 62]. In this study, our vaccine was associated with a decrease in BHBA (**Table 1**). However, in general, the *Salmonella*-based vaccine increased the levels of SCFAs in the feces of NOD mice.

Myristic, palmitic, and stearic acid are saturated fatty acids (SFAs) commonly found at high levels in individual with T1D [53]. SFAs stimulate the Toll-like receptor 4 (TLR-4) to increase pro-inflammatory cytokine expression [63]. Conversely, dicarboxylic acids with fatty acid substituents like succinic acid stimulated insulin biosynthesis [64], increased the secretion of pro-inflammatory cytokines such as TNFα and IL1β, and activated T cells [65, 66]. Herein, we found that vaccinated mice had decreased succinic acid (butanedioic acid). Medium and long chain unsaturated fatty acids such as azelaic, linoleic, oleic, octanoic, and pentadecanoic acid promote insulin secretion [67–70]. Also, these SFAs (succinic, palmitic, oleic, linoleic acids) were indirectly regulated by MYC (**S6C Fig**). Of note, inhibiting the medium and long chain fatty acid β-cell receptor (GPR40) impaired insulin secretion [71].

An increase in glutamate and a decrease in TCA metabolites were observed in diabetic NOD mice [72]. Our vaccinated mice showed a significant decrease in L-5-oxoproline (pyroglutamic acid) (**Table 1**). Vaccination was not associated with a change in the TCA metabolite, oxalic acid. Monoacylglycerol increased the glucagon-like peptide-1 (GLP-1) and gastric inhibitory polypeptide (GIP) levels following administration to the small intestine [73]. Our vaccine did not show effect on the abundance of monoacylglycerol (**Table 1**). Steroid metabolites in the gut of NOD mice were changed as a result of *Salmonella*-induced inflammation [74]. Steroids (cholesterol, coprostanol, stigmasterol, and campesterol) and eicosanoid can impact wound healing, sugar metabolism, and immune system regulation [74]. In fact, changes in cholesterol influenced multiple Disease and Functions pathways such as 'Concentration of ATP', 'Biosynthesis of amide', 'Synthesis of lipid' (**S6A Fig**), and 'Activation of leukocytes', 'Activation of phagocytes', and 'Inflammation of organ' (**S6B Fig**). Many of the metabolites assessed in the feces of vaccine-treated mice were altered over time. However,

analysis was not obtained on samples from unvaccinated mice. Hence, it is unknown if the changes in the metabolome were secondary to the vaccine alone.

In summary, we demonstrated that an oral *Salmonella* vaccine did not adversely alter gut microbiota diversity and proportions. At 30 days post-vaccination, the results suggested a transition in microbiota towards a more tolerant composition as the Tregs increased in mucosal tissues. Metabolic analysis indicated that after vaccination changes in metabolism, inflammation, and proliferation occurred and this was associated with immune activation and increased regulatory and decreased inflammatory cytokines. These results support the oral administration of *Salmonella* vaccines as carriers for autoantigens and immunomodulators against T1D. Further studies to understand the mechanistic role of the microbiota in immune function and to relate the composition of the microbiota to oral vaccines are required.

Supporting information

S1 Fig. Variation in fecal bacteria between vaccinated and vehicle-treated NOD mice. Abundance percentage of the fecal bacteria at the phylum level (A), genus level (B), and species level (C) in vaccine- (n = 25) and vehicle-treated (n = 25) mice.
(TIF)

S2 Fig. Variation in fecal mycoses between vaccinated and vehicle-treated NOD mice. Abundance percentage of the fecal mycoses at the phylum level (A), genus level (B), and species level (C) in vaccine- (n = 25) and vehicle-treated (n = 25) mice.
(TIF)

S3 Fig. Variation in fecal bacteria between vaccinated and vehicle-treated NOD mice. Abundance in percentage of the fecal bacteria at (A) the phylum level, and (B) genus level in the feces of NOD mice at time points pre-, 3-, 7-, 14-, and 30-days post-vaccination with oral *Salmonella*-based vaccine.
(TIF)

S4 Fig. Variation in fecal mycoses between vaccinated and vehicle-treated NOD mice. Abundance percentage of the fecal mycoses at (A) the phylum level, and (B) the genus level in NOD mice at different time points pre and 3-, 7-, 14-, and 30-days post-vaccination with oral *Salmonella*-based vaccine.
(TIF)

S5 Fig. Boxplots of changes in abundance percentage of the fecal mycoses at the phylum and genus levels. (A) The 4 most abundant phyla including *Ascomycota*, *Basidiomycota*, *Zygomycota*, *and Glomeromycota*. (B) The 4 most abundant genera included *Galactomyce*s, *Eurotium*, *Candida*, and *Geotrichum*. Each time point represents the mean ± SD of 4–6 samples. Group of vaccinated mice compared with vehicle treated at different time points. Mann-Whitney with Holm-Sidak correction for multiple comparisons test was used to report significance between groups at each time point using asterisks, *p < 0.05.
(TIF)

S6 Fig. The predicted pathways after vaccine administration. For each analysis, relevant metabolite measurements are located on the outside of the circle. The spokes leading to the center are the predicted relationship to the pathway which is in the center. Arrows on the spokes indicate that metabolite activates the pathway whereas bars indicate inhibition. **A) Disease and Functions: Molecular Functions**. Relative changes on days 3, 7, 14, and 30 in pathways Concentration of ATP, Biosynthesis of amide, Biosynthesis of hydrogen peroxide, and Synthesis of lipid. Legend of predicted measurements. **B) Disease and Functions: Immune**.

Relative changes on days 3, 7, 14, and 30 are indicated in pathways Activation of leukocytes, Activation of phagocytes, and Inflammation of organ. Legend of predicted measurements. **C**) **Upstream Regulators**. Relative changes in CPT1B, IL37, MYC, and MMP11 on days 3, 7, 14, and 30 are indicated. Legend of predicted measurements.
(ZIP)

Author Contributions

Conceptualization: Mohamed I. Husseiny.

Data curation: Jacob Cobb, Mauricio Retuerto, Janine C. Quijano, Mohamed I. Husseiny.

Formal analysis: Jacob Cobb, Sameh S. M. Soliman, Mauricio Retuerto, Chris Orr, Mohamed I. Husseiny.

Funding acquisition: Mohamed I. Husseiny.

Investigation: Mohamed I. Husseiny.

Methodology: Jacob Cobb, Sameh S. M. Soliman, Mauricio Retuerto, Mohamed I. Husseiny.

Project administration: Mohamed I. Husseiny.

Software: Chris Orr.

Supervision: Mahmoud Ghannoum, Fouad Kandeel, Mohamed I. Husseiny.

Validation: Jacob Cobb, Sameh S. M. Soliman, Mohamed I. Husseiny.

Visualization: Jacob Cobb, Mohamed I. Husseiny.

Writing – original draft: Jacob Cobb, Mohamed I. Husseiny.

Writing – review & editing: Sameh S. M. Soliman, Janine C. Quijano, Mahmoud Ghannoum, Fouad Kandeel, Mohamed I. Husseiny.

References

1. Nakayama M, Beilke JN, Jasinski JM, Kobayashi M, Miao D, Li M, et al. Priming and effector dependence on insulin B:9–23 peptide in NOD islet autoimmunity. The Journal of clinical investigation. 2007; 117(7):1835–43. Epub 2007/07/04. https://doi.org/10.1172/JCI31368 PMID: 17607359; PubMed Central PMCID: PMC1904318.

2. Achenbach P, Koczwara K, Knopff A, Naserke H, Ziegler AG, Bonifacio E. Mature high-affinity immune responses to (pro)insulin anticipate the autoimmune cascade that leads to type 1 diabetes. The Journal of clinical investigation. 2004; 114(4):589–97. Epub 2004/08/18. https://doi.org/10.1172/JCI21307 PMID: 15314696; PubMed Central PMCID: PMC503771.

3. Kronenberg D, Knight RR, Estorninho M, Ellis RJ, Kester MG, de Ru A, et al. Circulating preproinsulin signal peptide-specific CD8 T cells restricted by the susceptibility molecule HLA-A24 are expanded at onset of type 1 diabetes and kill beta-cells. Diabetes. 2012; 61(7):1752–9. Epub 2012/04/24. https://doi.org/10.2337/db11-1520 PMID: 22522618; PubMed Central PMCID: PMC3379678.

4. Skowera A, Ellis RJ, Varela-Calvino R, Arif S, Huang GC, Van-Krinks C, et al. CTLs are targeted to kill beta cells in patients with type 1 diabetes through recognition of a glucose-regulated preproinsulin epitope. The Journal of clinical investigation. 2008; 118(10):3390–402. Epub 2008/09/20. https://doi.org/10.1172/JCI35449 PMID: 18802479; PubMed Central PMCID: PMC2542849.

5. Husseiny MI, Rawson J, Kaye A, Nair I, Todorov I, Hensel M, et al. An oral vaccine for type 1 diabetes based on live attenuated Salmonella. Vaccine. 2014; 32(20):2300–7. https://doi.org/10.1016/j.vaccine.2014.02.070 PMID: 24631074.

6. Husseiny MI, Du W, Mbongue J, Lenz A, Rawson J, Kandeel F, et al. Factors affecting *Salmonella*-based combination immunotherapy for prevention of type 1 diabetes in non-obese diabetic mice. Vaccine. 2018. https://doi.org/10.1016/j.vaccine.2018.10.101 PMID: 30416020.

7. Mbongue JC, Rawson J, Garcia PA, Gonzalez N, Cobb J, Kandeel F, et al. Reversal of new onset type 1 diabetes by oral *Salmonella*-based combination therapy and mediated by regulatory T-cells in NOD mice. Frontiers in immunology. 2019; 10:320. https://doi.org/10.3389/fimmu.2019.00320 PMID: 30863412; PubMed Central PMCID: PMC6400227.

8. Husseiny MI, Wartha F, Hensel M. Recombinant vaccines based on translocated effector proteins of *Salmonella* Pathogenicity Island 2. Vaccine. 2007; 25(1):185–93.

9. Xiong G, Husseiny MI, Song L, Erdreich-Epstein A, Shackleford GM, Seeger RC, et al. Novel cancer vaccine based on genes of Salmonella pathogenicity island 2. International journal of cancer Journal international du cancer. 2010; 126(11):2622–34. https://doi.org/10.1002/ijc.24957 PMID: 19824039; PubMed Central PMCID: PMC2993175.

10. Xu X, Husseiny MI, Goldwich A, Hensel M. Efficacy of intracellular activated promoters for generation of *Salmonella*-based vaccines. Infection and immunity. 2010; 78(11):4828–38. https://doi.org/10.1128/IAI.00298-10 PMID: 20732994.

11. Cobb J, Rawson J, Gonzalez N, Hensel M, Kandeel F, Husseiny MI. Oral *Salmonella msbb* mutant as a carrier for a *Salmonella-based* vaccine for prevention and reversal of type 1 diabetes. Frontiers in immunology. 2021; 12:667897. Epub 2021/06/11. https://doi.org/10.3389/fimmu.2021.667897 PMID: 34108968; PubMed Central PMCID: PMC8181392.

12. Brenner FW, Villar RG, Angulo FJ, Tauxe R, Swaminathan B. Salmonella nomenclature. Journal of clinical microbiology. 2000; 38(7):2465–7. https://doi.org/10.1128/JCM.38.7.2465-2467.2000 PMID: 10878026; PubMed Central PMCID: PMC86943.

13. Abrahams GL, Hensel M. Manipulating cellular transport and immune responses: dynamic interactions between intracellular Salmonella enterica and its host cells. Cellular microbiology. 2006; 8(5):728–37. https://doi.org/10.1111/j.1462-5822.2006.00706.x PMID: 16611223.

14. Hensel M. *Salmonella* pathogenicity island 2. Mol Microbiol. 2000; 36(5):1015–23. Epub 2000/06/09. doi: mmi1935 [pii]. https://doi.org/10.1046/j.1365-2958.2000.01935.x PMID: 10844687.

15. Husseiny MI, Hensel M. Rapid method for the construction of *Salmonella enterica* Serovar Typhimurium vaccine carrier strains. Infection and immunity. 2005; 73(3):1598–605. https://doi.org/10.1128/IAI.73.3.1598–1605.2005 PMID: 15731059; PubMed Central PMCID: PMC1064926.

16. Husseiny MI, Hensel M. Evaluation of an intracellular-activated promoter for the generation of live *Salmonella* recombinant vaccines. Vaccine. 2005; 23(20):2580–90. https://doi.org/10.1016/j.vaccine.2004.11.035 PMID: 15780440.

17. Husseiny MI, Hensel M. Construction of highly attenuated *Salmonella enterica* serovar Typhimurium live vectors for delivering heterologous antigens by chromosomal integration. Microbiological research. 2008; 163(6):605–15. https://doi.org/10.1016/j.micres.2006.10.003 PMID: 19216101.

18. Husseiny MI, Hensel M. Evaluation of *Salmonella* live vaccines with chromosomal expression cassettes for translocated fusion proteins. Vaccine. 2009; 27(28):3780–7. https://doi.org/10.1016/j.vaccine.2009.03.053 PMID: 19464562.

19. Kong W, Brovold M, Koeneman BA, Clark-Curtiss J, Curtiss R 3rd., Turning self-destructing *Salmonella* into a universal DNA vaccine delivery platform. Proc Natl Acad Sci U S A. 2012; 109(47):19414–9. Epub 2012/11/07. https://doi.org/10.1073/pnas.1217554109 PMID: 23129620; PubMed Central PMCID: PMC3511069.

20. Yu X, Jia R, Huang J, Shu B, Zhu D, Liu Q, et al. Attenuated *Salmonella typhimurium* delivering DNA vaccine encoding duck enteritis virus UL24 induced systemic and mucosal immune responses and conferred good protection against challenge. Vet Res. 2012; 43(1):56. Epub 2012/07/10. https://doi.org/10.1186/1297-9716-43-56 PMID: 22770566; PubMed Central PMCID: PMC3412168.

21. Yang X, Xie L, Li YX, Wei CC. More than 9,000,000 Unique Genes in Human Gut Bacterial Community: Estimating Gene Numbers Inside a Human Body. Plos One. 2009; 4(6). doi: ARTN e6074 WOS:000267465900009. https://doi.org/10.1371/journal.pone.0006074 PMID: 19562079

22. Kamada N, Nunez G. Regulation of the immune system by the resident intestinal bacteria. Gastroenterology. 2014; 146(6):1477–88. Epub 2014/02/08. https://doi.org/10.1053/j.gastro.2014.01.060 PMID: 24503128; PubMed Central PMCID: PMC3995843.

23. Carding S, Verbeke K, Vipond DT, Corfe BM, Owen LJ. Dysbiosis of the gut microbiota in disease. Microb Ecol Health Dis. 2015; 26:26191. Epub 2015/02/06. https://doi.org/10.3402/mehd.v26.26191 PMID: 25651997; PubMed Central PMCID: PMC4315779.

24. Han H, Li Y, Fang J, Liu G, Yin J, Li T, et al. Gut Microbiota and Type 1 Diabetes. International journal of molecular sciences. 2018;19(4). https://doi.org/10.3390/ijms19040995 PMID: 29584630; PubMed Central PMCID: PMC5979537.

25. Mbongue JC, Alhoshani A, Rawson J, Garcia PA, Gonzalez N, Ferreri K, et al. Tracking of an oral *Salmonella*-based vaccine for type 1 diabetes in non-obese diabetic mice. Frontiers in immunology. 2020;

11:712. Epub 2020/05/16. https://doi.org/10.3389/fimmu.2020.00712 PMID: 32411136; PubMed Central PMCID: PMC7198770.

26. El Jurdi N, Filali-Mouhim A, Salem I, Retuerto M, Dambrosio NM, Baer L, et al. Gastrointestinal Microbiome and Mycobiome Changes during Autologous Transplantation for Multiple Myeloma: Results of a Prospective Pilot Study. Biology of blood and marrow transplantation: journal of the American Society for Blood and Marrow Transplantation. 2019; 25(8):1511–9. https://doi.org/10.1016/j.bbmt.2019.04.007 PMID: 30959164.

27. Soliman SSM, Alhamidi TB, Abdin S, Almehdi AM, Semreen MH, Alhumaidi RB, et al. Effective targeting of breast cancer cells (MCF7) via novel biogenic synthesis of gold nanoparticles using cancer-derived metabolites. PloS one. 2020; 15(10):e0240156. https://doi.org/10.1371/journal.pone.0240156 PMID: 33022008

28. Soliman S, Mohammad MG, El-Keblawy AA, Omar H, Abouleish M, Madkour M, et al. Mechanical and phytochemical protection mechanisms of Calligonum comosum in arid deserts. PloS one. 2018; 13(2): e0192576. https://doi.org/10.1371/journal.pone.0192576 PMID: 29415032

29. Rossetti M, Spreafico R, Saidin S, Chua C, Moshref M, Leong JY, et al. Ex vivo-expanded but not in vitro-induced human regulatory T cells are candidates for cell therapy in autoimmune diseases thanks to stable demethylation of the FOXP3 regulatory T cell-specific demethylated region. J Immunol. 2015; 194(1):113–24. https://doi.org/10.4049/jimmunol.1401145 PMID: 25452562; PubMed Central PMCID: PMC4383769.

30. Su Z, Tao X. Current Understanding of IL-37 in Human Health and Disease. Frontiers in immunology. 2021; 12:696605. Epub 2021/07/13. https://doi.org/10.3389/fimmu.2021.696605 PMID: 34248996; PubMed Central PMCID: PMC8267878.

31. Ronchi JA, Figueira TR, Ravagnani FG, Oliveira HC, Vercesi AE, Castilho RF. A spontaneous mutation in the nicotinamide nucleotide transhydrogenase gene of C57BL/6J mice results in mitochondrial redox abnormalities. Free Radic Biol Med. 2013; 63:446–56. Epub 2013/06/12. https://doi.org/10.1016/j.freeradbiomed.2013.05.049 PMID: 23747984.

32. Evans RM, Barish GD, Wang YX. PPARs and the complex journey to obesity. Nat Med. 2004; 10 (4):355–61. Epub 2004/04/02. https://doi.org/10.1038/nm1025 PMID: 15057233.

33. Rufer AC, Thoma R, Hennig M. Structural insight into function and regulation of carnitine palmitoyltransferase. Cell Mol Life Sci. 2009; 66(15):2489–501. https://doi.org/10.1007/s00018-009-0035-1 WOS:000268102000006. PMID: 19430727

34. Hughes D, Guttenplan JB, Marcus CB, Subbaramaiah K, Dannenberg AJ. Heat Shock Protein 90 Inhibitors Suppress Aryl Hydrocarbon Receptor-Mediated Activation of CYP1A1 and CYP1B1 Transcription and DNA Adduct Formation. Cancer Prev Res. 2008; 1(6):485–93. https://doi.org/10.1158/1940-6207.CAPR-08-0149 WOS:000264293900013. PMID: 19138996

35. Ahmadi SE, Rahimi S, Zarandi B, Chegeni R, Safa M. Correction to: MYC: a multipurpose oncogene with prognostic and therapeutic implications in blood malignancies. J Hematol Oncol. 2021; 14(1):135. Epub 2021/09/04. https://doi.org/10.1186/s13045-021-01152-9 PMID: 34474678; PubMed Central PMCID: PMC8414674.

36. Kressler D, Schreiber SN, Knutti D, Kralli A. The PGC-1-related protein PERC is a selective coactivator of estrogen receptor alpha. J Biol Chem. 2002; 277(16):13918–25. https://doi.org/10.1074/jbc.M201134200 WOS:000175096000075. PMID: 11854298

37. Wolkow CA, Iser WB. Uncoupling protein homologs may provide a link between mitochondria, metabolism and lifespan. Ageing Res Rev. 2006; 5(2):196–208. https://doi.org/10.1016/j.arr.2006.03.007 WOS:000238333200006. PMID: 16707280

38. Furuhashi M, Saitoh S, Shimamoto K, Miura T. Fatty Acid-Binding Protein 4 (FABP4): Pathophysiological Insights and Potent Clinical Biomarker of Metabolic and Cardiovascular Diseases. Clin Med Insights Cardiol. 2014; 8(Suppl 3):23–33. Epub 2015/02/13. https://doi.org/10.4137/CMC.S17067 PMID: 25674026; PubMed Central PMCID: PMC4315049.

39. Kang SU, Cho SY, Jeong H, Han J, Chae HY, Yang H, et al. Matrix metalloproteinase 11 (MMP11) in macrophages promotes the migration of HER2-positive breast cancer cells and monocyte recruitment through CCL2-CCR2 signaling. Lab Invest. 2022; 102(4):376–90. Epub 2021/11/15. https://doi.org/10.1038/s41374-021-00699-y PMID: 34775491

40. Paton CM, Ntambi JM. Biochemical and physiological function of stearoyl-CoA desaturase. Am J Physiol Endocrinol Metab. 2009; 297(1):E28–37. Epub 2008/12/11. https://doi.org/10.1152/ajpendo.90897.2008 PMID: 19066317; PubMed Central PMCID: PMC2711665.

41. Costello EK, Stagaman K, Dethlefsen L, Bohannan BJ, Relman DA. The application of ecological theory toward an understanding of the human microbiome. Science. 2012; 336(6086):1255–62. https://doi.org/10.1126/science.1224203 PMID: 22674335; PubMed Central PMCID: PMC4208626.

42. Lupp C, Robertson ML, Wickham ME, Sekirov I, Champion OL, Gaynor EC, et al. Host-mediated inflammation disrupts the intestinal microbiota and promotes the overgrowth of Enterobacteriaceae. Cell host & microbe. 2007; 2(3):204. https://doi.org/10.1016/j.chom.2007.08.002 PMID: 18030708.

43. Barman M, Unold D, Shifley K, Amir E, Hung K, Bos N, et al. Enteric salmonellosis disrupts the microbial ecology of the murine gastrointestinal tract. Infection and immunity. 2008; 76(3):907–15. https://doi.org/10.1128/IAI.01432-07 PMID: 18160481; PubMed Central PMCID: PMC2258829.

44. Wen L, Ley RE, Volchkov PY, Stranges PB, Avanesyan L, Stonebraker AC, et al. Innate immunity and intestinal microbiota in the development of type 1 diabetes. Nature. 2008; 455(7216):1109–U10. https://doi.org/10.1038/nature07336 WOS:000260252600045. PMID: 18806780

45. Burrows MP, Volchkov P, Kobayashi KS, Chervonsky AV. Microbiota regulates type 1 diabetes through Toll-like receptors. Proceedings of the National Academy of Sciences of the United States of America. 2015; 112(32):9973–7. https://doi.org/10.1073/pnas.1508740112 WOS:000359285100062. PMID: 26216961

46. Pearson JA, Wong FS, Wen L. The importance of the Non Obese Diabetic (NOD) mouse model in autoimmune diabetes. J Autoimmun. 2016; 66:76–88. https://doi.org/10.1016/j.jaut.2015.08.019 PMID: 26403950; PubMed Central PMCID: PMC4765310.

47. Tanase DM, Gosav EM, Neculae E, Costea CF, Ciocoiu M, Hurjui LL, et al. Role of Gut Microbiota on Onset and Progression of Microvascular Complications of Type 2 Diabetes (T2DM). Nutrients. 2020; 12 (12). Epub 2020/12/06. https://doi.org/10.3390/nu12123719 PMID: 33276482; PubMed Central PMCID: PMC7760723.

48. Groschwitz KR, Hogan SP. Intestinal barrier function: molecular regulation and disease pathogenesis. J Allergy Clin Immunol. 2009; 124(1):3–20; quiz 1–2. https://doi.org/10.1016/j.jaci.2009.05.038 PMID: 19560575; PubMed Central PMCID: PMC4266989.

49. Valladares R, Sankar D, Li N, Williams E, Lai KK, Abdelgeliel AS, et al. *Lactobacillus johnsonii* N6.2 mitigates the development of type 1 diabetes in BB-DP rats. PloS one. 2010; 5(5):e10507. Epub 2010/05/14. https://doi.org/10.1371/journal.pone.0010507 PMID: 20463897; PubMed Central PMCID: PMC2865539.

50. Neu J, Reverte CM, Mackey AD, Liboni K, Tuhacek-Tenace LM, Hatch M, et al. Changes in intestinal morphology and permeability in the BioBreeding rat before the onset of type 1 diabetes. Journal of Pediatric Gastroenterology and Nutrition. 2005; 40(5):589–95. https://doi.org/10.1097/01.mpg.0000159636.19346.c1 WOS:000228846900012. PMID: 15861021

51. Yan-Do R, MacDonald PE. Impaired "Glycine"-mia in Type 2 Diabetes and Potential Mechanisms Contributing to Glucose Homeostasis. Endocrinology. 2017; 158(5):1064–73. Epub 2017/03/23. https://doi.org/10.1210/en.2017-00148 PMID: 28323968.

52. Wishart DS, Feunang YD, Marcu A, Guo AC, Liang K, Vazquez-Fresno R, et al. HMDB 4.0: the human metabolome database for 2018. Nucleic Acids Res. 2018; 46(D1):D608–D17. Epub 2017/11/16. https://doi.org/10.1093/nar/gkx1089 PMID: 29140435; PubMed Central PMCID: PMC5753273.

53. Arneth B, Arneth R, Shams M. Metabolomics of Type 1 and Type 2 Diabetes. Int J Mol Sci. 2019; 20 (10). Epub 2019/05/22. https://doi.org/10.3390/ijms20102467 PMID: 31109071; PubMed Central PMCID: PMC6566263.

54. Vangipurapu J, Stancakova A, Smith U, Kuusisto J, Laakso M. Nine Amino Acids Are Associated With Decreased Insulin Secretion and Elevated Glucose Levels in a 7.4-Year Follow-up Study of 5,181 Finnish Men. Diabetes. 2019; 68(6):1353–8. Epub 2019/03/20. https://doi.org/10.2337/db18-1076 PMID: 30885989.

55. Wang SP, Rubio LA, Duncan SH, Donachie GE, Holtrop G, Lo G, et al. Pivotal Roles for pH, Lactate, and Lactate-Utilizing Bacteria in the Stability of a Human Colonic Microbial Ecosystem. mSystems. 2020; 5(5). Epub 2020/09/10. https://doi.org/10.1128/mSystems.00645-20 PMID: 32900872; PubMed Central PMCID: PMC7483512.

56. Tan J, McKenzie C, Potamitis M, Thorburn AN, Mackay CR, Macia L. The role of short-chain fatty acids in health and disease. Adv Immunol. 2014; 121:91–119. https://doi.org/10.1016/B978-0-12-800100-4.00003-9 PMID: 24388214.

57. Albenberg LG, Wu GD. Diet and the intestinal microbiome: associations, functions, and implications for health and disease. Gastroenterology. 2014; 146(6):1564–72. Epub 2014/02/08. https://doi.org/10.1053/j.gastro.2014.01.058 PMID: 24503132; PubMed Central PMCID: PMC4216184.

58. Maslowski KM, Vieira AT, Ng A, Kranich J, Sierro F, Yu D, et al. Regulation of inflammatory responses by gut microbiota and chemoattractant receptor GPR43. Nature. 2009; 461(7268):1282–6. Epub 2009/10/30. https://doi.org/10.1038/nature08530 PMID: 19865172; PubMed Central PMCID: PMC3256734.

59. Florowska A, Krygier K, Florowski T, Dluzewska E. Prebiotics as functional food ingredients preventing diet-related diseases. Food Funct. 2016; 7(5):2147–55. https://doi.org/10.1039/c5fo01459j WOS:000377136900002. PMID: 26961814

60. Sun J, Furio L, Mecheri R, van der Does AM, Lundeberg E, Saveanu L, et al. Pancreatic beta-Cells Limit Autoimmune Diabetes via an Immunoregulatory Antimicrobial Peptide Expressed under the Influence of the Gut Microbiota. Immunity. 2015; 43(2):304–17. Epub 2015/08/09. https://doi.org/10.1016/j.immuni.2015.07.013 PMID: 26253786.

61. Taboulet P, Deconinck N, Thurel A, Haas L, Manamani J, Porcher R, et al. Correlation between urine ketones (acetoacetate) and capillary blood ketones (3-beta-hydroxybutyrate) in hyperglycaemic patients. Diabetes Metab. 2007; 33(2):135–9. https://doi.org/10.1016/j.diabet.2006.11.006 PMID: 17320448.

62. Klocker AA, Phelan H, Twigg SM, Craig ME. Blood beta-hydroxybutyrate vs. urine acetoacetate testing for the prevention and management of ketoacidosis in Type 1 diabetes: a systematic review. Diabet Med. 2013; 30(7):818–24. https://doi.org/10.1111/dme.12136 PMID: 23330615.

63. Chueire VB, Muscelli E. Effect of free fatty acids on insulin secretion, insulin sensitivity and incretin effect—a narrative review. Arch Endocrinol Metab. 2021; 65(1):24–31. Epub 2020/12/16. https://doi.org/10.20945/2359-3997000000313 PMID: 33320449.

64. Alarcon C, Wicksteed B, Prentki M, Corkey BE, Rhodes CJ. Succinate is a preferential metabolic stimulus-coupling signal for glucose-induced proinsulin biosynthesis translation. Diabetes. 2002; 51 (8):2496–504. https://doi.org/10.2337/diabetes.51.8.2496 WOS:000177185900021. PMID: 12145163

65. Gilissen J, Jouret F, Pirotte B, Hanson J. Insight into SUCNR1 (GPR91) structure and function. Pharmacology & Therapeutics. 2016; 159:56–65. https://doi.org/10.1016/j.pharmthera.2016.01.008 WOS:000372773600004. PMID: 26808164

66. Mills E O'Neill LA. Succinate: a metabolic signal in inflammation. Trends Cell Biol. 2014; 24(5):313–20. https://doi.org/10.1016/j.tcb.2013.11.008 PMID: 24361092.

67. Fu WC, Li HY, Li TT, Yang K, Chen JX, Wang SJ, et al. Pentadecanoic acid promotes basal and insulin-stimulated glucose uptake in C2C12 myotubes. Food Nutr Res. 2021;65. Epub 2021/02/23. https://doi.org/10.29219/fnr.v65.4527 PMID: 33613155; PubMed Central PMCID: PMC7869443.

68. Zhang T, Chen P, Stanley CA, Hoshi T, Li C. Mechanisms of octanoic acid potentiation of insulin secretion in isolated islets. Islets. 2019; 11(4):77–88. Epub 2019/03/09. https://doi.org/10.1080/19382014.2019.1566683 PMID: 30849280; PubMed Central PMCID: PMC6682262.

69. Zong G, Liu G, Willett WC, Wanders AJ, Alssema M, Zock PL, et al. Associations Between Linoleic Acid Intake and Incident Type 2 Diabetes Among US Men and Women. Diabetes Care. 2019; 42(8):1406–13. https://doi.org/10.2337/dc19-0412 WOS:000476786200012. PMID: 31182488

70. Muthulakshmi S, Saravanan R. Efficacy of azelaic acid on hepatic key enzymes of carbohydrate metabolism in high fat diet induced type 2 diabetic mice. Biochimie. 2013; 95(6):1239–44. Epub 2013/02/14. https://doi.org/10.1016/j.biochi.2013.01.018 PMID: 23402910.

71. Meidute Abaraviciene S, Muhammed SJ, Amisten S, Lundquist I, Salehi A. GPR40 protein levels are crucial to the regulation of stimulated hormone secretion in pancreatic islets. Lessons from spontaneous obesity-prone and non-obese type 2 diabetes in rats. Mol Cell Endocrinol. 2013; 381(1–2):150–9. Epub 2013/08/06. https://doi.org/10.1016/j.mce.2013.07.025 PMID: 23911664.

72. Madsen R, Banday VS, Moritz T, Trygg J, Lejon K. Altered metabolic signature in pre-diabetic NOD mice. PLoS One. 2012; 7(4):e35445. https://doi.org/10.1371/journal.pone.0035445 PMID: 22514744; PubMed Central PMCID: PMC3326011.

73. Hansen KB, Rosenkilde MM, Knop FK, Wellner N, Diep TA, Rehfeld JF, et al. 2-Oleoyl Glycerol Is a GPR119 Agonist and Signals GLP-1 Release in Humans. J Clin Endocr Metab. 2011; 96(9):E1409–E17. https://doi.org/10.1210/jc.2011-0647 WOS:000294558600007. PMID: 21778222

74. Ahmer BM, Gunn JS. Interaction of Salmonella spp. with the Intestinal Microbiota. Front Microbiol. 2011; 2:101. Epub 2011/07/21. https://doi.org/10.3389/fmicb.2011.00101 PMID: 21772831; PubMed Central PMCID: PMC3131049.